

# Reports

## Neptune's Wind Speeds Obtained by Tracking Clouds in Voyager Images

H. B. HAMMEL,\* R. F. BEEBE, E. M. DE JONG, C. J. HANSEN, C. D. HOWELL, A. P. INGERSOLL, T. V. JOHNSON, S. S. LIMAYE, J. A. MAGALHÃES, J. B. POLLACK, L. A. SROMOVSKY, V. E. SUOMI, C. E. SWIFT

Images of Neptune obtained by the narrow-angle camera of the Voyager 2 spacecraft reveal large-scale cloud features that persist for several months or longer. The features' periods of rotation about the planetary axis range from 15.8 to 18.4 hours. The atmosphere equatorward of  $-53^\circ$  rotates with periods longer than the 16.05-hour period deduced from Voyager's planetary radio astronomy experiment (presumably the planet's internal rotation period). The wind speeds computed with respect to this radio period range from 20 meters per second eastward to 325 meters per second westward. Thus, the cloud-top wind speeds are roughly the same for all the planets ranging from Venus to Neptune, even though the solar energy inputs to the atmospheres vary by a factor of 1000.

THE VOYAGER 2 SPACECRAFT IS JUST now completing its grand tour of the outer solar system. Early Voyager images of Neptune have revealed previously unseen atmospheric features. We have tracked these discrete cloud features in images obtained over a 65-day period from 10 June to 13 August 1989. We combine these with ground-based results to generate a zonal velocity profile for the atmosphere. The wind speeds establish the basic characteristics of the cloud-level circulation in the southern hemisphere of Neptune.

Ground-based telescopic observations of Neptune have revealed evidence of discrete bright features, both in images of the planet (1-3) and in disk-integrated photometric observations, which showed periodic variability (4-6). Most of the ground-based data were obtained at wavelengths longer than  $8000 \text{ \AA}$ , where the contrast between bright features and the surrounding atmosphere is large. Recent images at  $6190 \text{ \AA}$  also have revealed discrete features and a bright polar

region (3). But even the best ground-based images showed no latitudinal banding or dark features (2). The latitudes of the brightest features differed from year to year (3). The brightest cloud feature detected in ground-based imaging in 1986 and 1987 was located at  $-39^\circ \pm 3^\circ$  and had a rotation period of 17.0 hours (5, 7). The brightest feature in 1988 was located at  $-31^\circ \pm 3^\circ$  and had a rotation period of 17.7 hours (3, 6). All latitudes quoted in this paper are planetographic (8).

Figure 1 shows some of the discrete features visible in narrow-angle Voyager images taken on 25 and 26 July 1989, exactly 1 month before the closest approach to Neptune. Contrast is on the order of 10% for all six camera filters, although the appearance of the planet differs from ultraviolet to orange. Features are named according to the planetographic latitude at which they were first detected (Fig. 1C). Thus S22 is the large dark oval centered at  $-22^\circ$  latitude. It is informally known as the Great Dark Spot (GDS) because it resembles the Great Red Spot of Jupiter. The resemblance is remarkable in general shape, relative size, and position on the planet. For both Jupiter and Neptune, the great spots cover approximately  $15^\circ$  in latitude by  $30^\circ$  in longitude, occupy stable positions in latitude bands centered near  $-22^\circ$ , and are associated with bright, active regions (9). The bright companion immediately to the south of S22 and the bright streamer to the east were the first features seen on Neptune by Voyager 2 (initially detected in January 1989). The companion is most likely the bright cloud feature seen in the low-resolution ground-based images (3) because it is prominent at the longest wavelengths of the Voyager cameras and occurs at the appropriate latitude,  $-33^\circ$ . It has remained at the same longitude as S22.

After the discovery of the GDS (S22) and its long-term companion, a bright polar feature (S71) was discovered in June 1989. The fast-moving "Scooter" (S42) was discovered soon thereafter, followed by a second dark feature (S54) that is now known simply as D2. These four long-lived features form the basis of our zonal velocity measure-

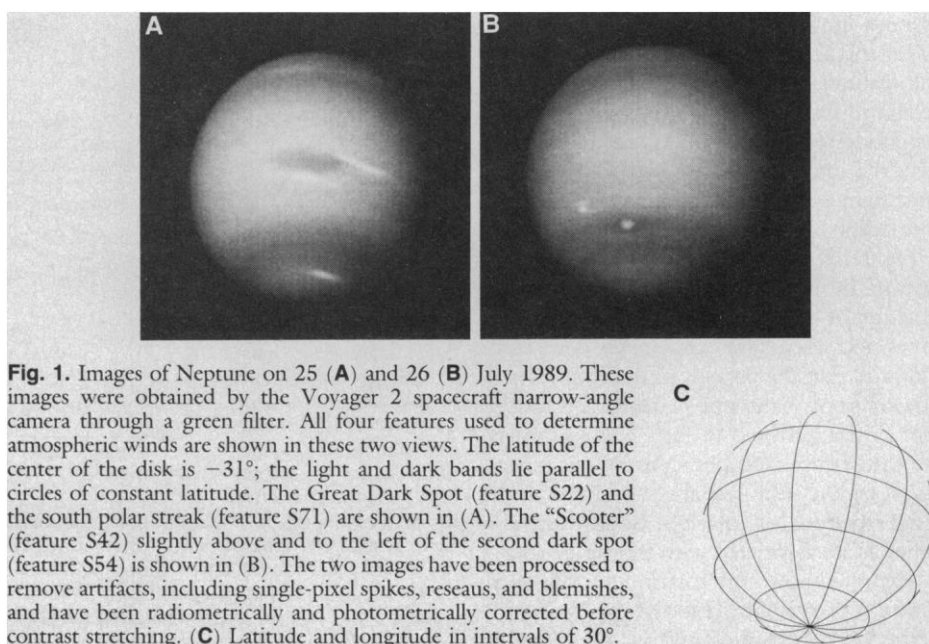


Fig. 1. Images of Neptune on 25 (A) and 26 (B) July 1989. These images were obtained by the Voyager 2 spacecraft narrow-angle camera through a green filter. All four features used to determine atmospheric winds are shown in these two views. The latitude of the center of the disk is  $-31^\circ$ ; the light and dark bands lie parallel to circles of constant latitude. The Great Dark Spot (feature S22) and the south polar streak (feature S71) are shown in (A). The "Scooter" (feature S42) slightly above and to the left of the second dark spot (feature S54) is shown in (B). The two images have been processed to remove artifacts, including single-pixel spikes, reseaus, and blemishes, and have been radiometrically and photometrically corrected before contrast stretching. (C) Latitude and longitude in intervals of  $30^\circ$ .

H. B. Hammel, C. J. Hansen, T. V. Johnson, Jet Propulsion Laboratory, California Institute of Technology, Pasadena, CA 91109.

R. F. Beebe, New Mexico State University, Las Cruces, NM 88003.

E. M. De Jong, C. D. Howell, A. P. Ingersoll, C. E. Swift, California Institute of Technology, Pasadena, CA 91125.

S. S. Limaye, L. A. Sromovsky, V. E. Suomi, University of Wisconsin-Madison, Madison, WI 53706.

J. A. Magalhães, Stanford University, Stanford, CA 94305.

J. B. Pollack, NASA/Ames Research Center, Moffett Field, CA 94035.

\*To whom correspondence should be addressed.

ments. Appearance and disappearance of ephemeral bright streamers at the latitude of S22 and at  $+25^\circ$  provides further evidence of temporal variability in Neptune's atmosphere.

Our analysis is limited to large, long-lived features in the southern hemisphere. The center of the planet's disk in our images is at approximately  $-31^\circ$  (see Fig. 1C) and the solar illumination is centered at approximately  $-27^\circ$  (10). Thus, we have a bias toward detecting features in the southern mid-latitudes of Neptune's atmosphere, although we see bright structure as far north as  $+25^\circ$  (Fig. 1). Similar structures in the equatorial region would be detectable, but none were seen. Images obtained after 13 August 1989 may reveal small-scale features at all latitudes. But we do not anticipate changes in our estimates of the long-term motions of the largest features, because our observation interval includes most of the long baseline observations that Voyager made.

In our analysis, we used 125 clear-filter and 90 orange-filter images. These filters were chosen because they provided the highest number of images with good feature contrast. Orange provided high contrast for brighter features; clear showed high contrast for darker features. The images in Fig. 1 are representative of the highest resolution images in our sample; we used green-filter images, a compromise between the orange and clear images, to show good contrast for both bright and dark features.

Several steps were involved in determining the latitude and longitude of specific features (11, 12). The position of the planet's center was calculated by projecting an oblate spheroid onto the camera image plane and iteratively determining the best fit to the planet's limb. We then computed the latitudes and longitudes of selected points on the features. We chose a separate rotating reference frame for each feature so that its longitude remained approximately constant over the interval of observation. The reference frames rotate uniformly and are therefore defined by their periods of rotation (7).

Figure 2 shows the longitude of each feature in its own reference frame as a function of time. That the longitudes sometimes increased and sometimes decreased indicates that the periods of the features are not constant. Constant periods of rotation plot as straight lines in Fig. 2. Also shown are the feature latitudes. Northward excursions of the features are associated with longer periods of rotation. Southward excursions are associated with shorter periods.

Figure 3 shows the rotation periods as a function of latitude. Three of the Voyager-derived features are plotted at two different

latitudes, each with its own observed period. The fourth feature, S71, is so variable that it was plotted only at its average latitude. The periods for features that are evident in the ground-based images and whose latitudes are known are also plotted (3, 5, 6); the range of periods for features for which latitudes are not known, 17.7 to 18.2 hours (4), is consistent with the range of mid-latitude periods.

Several interesting conclusions emerge from the data in Fig. 3. First, the measured periods generally decrease from low southern latitudes (S22) to high southern latitudes (S71), although the shortest period of rotation (15.8 hours) occurs at  $-55^\circ$ . Second, the change in period with latitude for single features generally falls along the curve defined by the different features. Finally, the periods of the ground-based data for 1986 to 1988 agree quite well with the Voyager data for 1989.

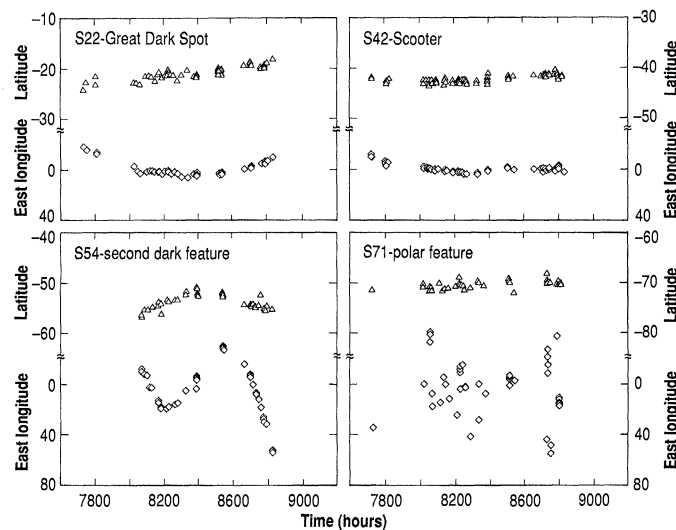
Figure 3 also shows the zonal velocities relative to the 16.05-hour period derived from the planetary radio astronomy experiment on Voyager (13). The radio emissions are probably controlled by the magnetic field and therefore should reflect the rotation of Neptune's interior. As shown in Fig. 3, most of the atmosphere (equatorward of  $-53^\circ$ ) has longer periods of rotation than the radio period. The GDS appears to move westward at speeds up to 325 m/s relative to Neptune's interior. Westward flow also occurs in the equatorial regions of Earth and Uranus (14), but the wind speeds are lower than those seen on Neptune. The magnitude of Neptune's equatorial flow inferred from

the motion of the GDS is second only to the 500 m/s eastward equatorial jet of Saturn (15). That the winds are of the order 100 m/s on all the planets ranging from Venus to Neptune, even though the solar energy input varies by a factor of 1000, is a challenge that any theory of atmospheric dynamics must face.

With its distinct large-scale features and obvious banding, Neptune's cloud patterns resemble those on Jupiter more than they resemble those on Saturn or Uranus, although all the giant planets are distinguished by large-scale parallel cloud bands, long-lived features, and small-scale temporal variability (9, 14, 15). This resemblance is puzzling because there is so little energy available at Neptune. For instance, the power per unit area (absorbed sunlight plus internal heating) on Neptune is about 5% of that available on Jupiter.

Another puzzling observation, possibly related to the first, is the high degree of predictability of the positions of large-scale features in the giant planet atmospheres. Voyager command sequences are "frozen" 10 days before they are executed. This delay means that a 10-day "weather forecast" is required if one wishes to image the interesting features at high resolution during the final days before closest approach. Such weather forecasts have been enormously successful during all the Voyager encounters (9, 14, 15). Our study, based on 65 days of Neptune observations, indicates that the same type of forecast will work for most features on Neptune, even though different features move at different rates and make

**Fig. 2.** Latitude ( $\Delta$ ) and longitude ( $\diamond$ ) (in degrees) as a function of time (in hours) for the four features tracked in the Voyager images. The measured longitude of each feature is plotted in the feature's own reference frame, which is defined by the constant period of rotation (7) that approximately minimizes its excursion in longitude. (A) The latitudes and longitudes of S22 (the Great Dark Spot) relative to an 18.33-hour period; (B) the same for the "Scooter" (S42) relative to a 16.76-hour period; (C) for the second dark spot (S54) relative to 16.07 hours; (D) for the south polar feature and 15.97 hours. Generally the slope of each longitude curve is greatest (longest period of rotation) when the latitude of the feature is largest (maximum northward excursion). Camera shuttering time is indicated along the abscissa in hours and is 0.8 times the spacecraft flight data system (FDS) count. Thus, 8800 hours corresponds to 3.71 hours UT on 12 August 1989. At this time the longitudinal positions (degrees west of the subspacecraft meridian) of S22, S42, S54, S71, and the subsolar point were  $220.1^\circ$ ,  $302.1^\circ$ ,  $213.9^\circ$ ,  $32.7^\circ$ , and  $15.7^\circ$ , respectively.



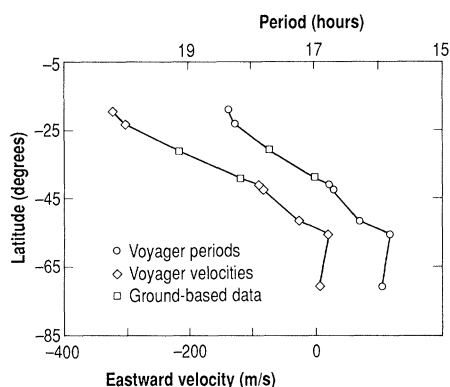


**Fig. 3.** Zonal velocity ( $\diamond$ ) and atmospheric rotation period ( $\circ$ ) as a function of latitude for long-lived features in the atmosphere of Neptune. The upper axis shows atmospheric rotation periods (7). The lower axis indicates eastward velocity relative to a uniform rotation period of 16.05 hours, the radio rotation period (13). Points indicated by squares were obtained from ground-based observations; all other points were derived from spacecraft images. Some features were measured at two different latitudes. The points are connected by lines merely to clarify the diagram; higher resolution data may reveal additional structure.

many rotations over the time of extrapolation. For instance, S54 made 15.19 rotations while S22 made 13.11 rotations in the same 10-day interval.

Wind is perhaps the most fundamental variable in dynamic meteorology, yet there is no unified theory that accounts for the wind speeds observed in all planetary atmospheres. Two decades ago, the importance of planetary rotations in organizing planetary flows was not anticipated. Over the years Voyager wind observations revealed many surprises, including the high-velocity, localized winds in the midst of Jupiter's long-lived large features (9), the high wind speed at Saturn's equator relative to the interior (15), and the dominance of east-west winds at Uranus despite that planet's peculiar orientation (14). The resemblance to the other giant planets is probably just the first of Neptune's surprises. The only sure lesson in the science of comparative planetology is humility.

#### REFERENCES AND NOTES

1. B. A. Smith, H. J. Reitsema, S. M. Larson, *Bull. Am. Astron. Soc.* **11**, 570 (1979); R. J. Terrile and B. A. Smith, *ibid.* **15**, 858 (1983); J. N. Heasley, *Publ. Astron. Soc. Pac.* **96**, 767 (1984); —, C. B. Pilcher, R. R. Howell, J. J. Caldwell, *Icarus* **57**, 432 (1984); B. A. Smith, in *Uranus and Neptune*, J. T. Bergstralh, Ed. (NASA Conf. Publ. 2330, National Aeronautics and Space Administration, Houston, 1984), pp. 213–223; M. J. S. Belton and R. Terrile, *ibid.*, pp. 327–347; H. B. Hammel and M. W. Buie, *Icarus* **72**, 62 (1987).
2. H. B. Hammel, thesis, University of Hawaii at Manoa (1988); *Icarus* **80**, 14 (1989).
3. —, *Science* **244**, 1165 (1989).
4. D. Slavsky and H. J. Smith, *Astrophys. J.* **226**, L49 (1978); H. J. Smith and D. Slavsky, *Bull. Am. Astron. Soc.* **12**, 704 (1980); M. J. S. Belton, L.

Wallace, S. Howard, *Icarus* **46**, 263 (1981); R. H. Brown, D. P. Cruikshank, A. T. Tokunaga, *ibid.* **47**, 159 (1981).

5. H. B. Hammel et al., *Icarus* **79**, 1 (1989).
6. H. B. Hammel and J. Harrington, in preparation.
7. A rotation period is defined as the time interval between successive crossings of a reference meridian that is tied to a nonrotating (inertial) coordinate system.
8. The ground-based latitudes were originally measured in a planetocentric coordinate system and have been converted to a planetographic system. Planetocentric latitude is the elevation angle of a line from a planet's center relative to the planet's equatorial plane. Planetographic latitude is the elevation angle of the normal to the planet's surface relative to the planet's equatorial plane. The two latitudes are identical for a spherical body; Neptune's oblateness leads to a difference of less than  $1^\circ$  between the two systems.
9. B. M. Peek, *The Planet Jupiter* (Faber and Faber, London, revised ed., 1981), chap. 9; B. A. Smith and G. E. Hunt, in *Jupiter*, T. Gehrels, Ed. (Univ. of Arizona Press, Tucson, 1976), pp. 564–585; B. A. Smith et al., *Science* **204**, 951 (1979); B. A. Smith et al., *ibid.* **206**, 927 (1979).
10. The phase angle (the angle between the sun, the planet, and the spacecraft) was  $15^\circ$ .
11. In our measurements we used raw images in order to

avoid artifacts that are introduced by image processing.

12. We used the program NAV, which was developed by G. Yagi at the Multimission Image Processing Laboratory (MIPL), Jet Propulsion Laboratory, California Institute of Technology, in consultation with one of us (A.P.I.). An independent set of similar calculations was performed at the University of Wisconsin–Madison, confirming our calculations.
13. J. W. Warwick et al., Voyager press conference at the Jet Propulsion Laboratory, Pasadena, CA, 27 August 1989; J. W. Warwick et al., in preparation.
14. B. A. Smith et al., *Science* **233**, 43 (1986).
15. B. A. Smith et al., *ibid.* **213**, 163 (1981); B. A. Smith et al., *ibid.* **215**, 504 (1982).
16. This research was supported by NASA, primarily through the Voyager Project Office at the Jet Propulsion Laboratory (JPL), California Institute of Technology (Caltech). H.B.H. acknowledges the support of a National Research Council Resident Research Associateship, sponsored by JPL-Caltech, through an agreement with NASA. We thank D. Hinson for pointing out an error in the preliminary calculations. We also thank D. A. Alexander, L. Wynn, and G. W. Garneau for processing and preparation of the photos.

4 August 1989; accepted 17 August 1989

## Negative Differential Resistance on the Atomic Scale: Implications for Atomic Scale Devices

IN-WHAN LYO AND PHAEDON AVOURIS

Negative differential resistance (NDR) is the essential property that allows fast switching in certain types of electronic devices. With scanning tunneling microscopy (STM) and scanning tunneling spectroscopy, it is shown that the current-voltage characteristics of a diode configuration consisting of an STM tip over specific sites of a boron-exposed silicon(111) surface exhibit NDR. These NDR-active sites are of atomic dimensions ( $\sim 1$  nanometer). NDR in this case is the result of tunneling through localized, atomic-like states. Thus, desirable device characteristics can be obtained even on the atomic scale.

THERE HAS BEEN A CONTINUING EFFORT to decrease the dimensions and to understand the size limitations of microelectronic devices. At small dimensions, most conventional device structures face fundamental and technological limitations. At very small dimensions characteristic quantum effects become prominent, which, while placing limits on the size of conventional devices, can be exploited to create a new class of quantum effect devices such as quantum wells and their one- and zero-dimensional analogs, quantum wires and quantum dots (1). Another device that exploits quantum effects, electron tunneling in particular, is the Esaki diode (2). A common characteristic of both types of quantum effect devices, that is, Esaki diodes and quantum-well type structures, is the presence of regions of NDR in their curves

of current versus voltage ( $I$ - $V$ ). NDR, which is the phenomenon of decreasing current with increasing voltage, is the essential property that allows such devices to be used as fast switches, oscillators, and frequency-locking circuits (1, 3).

In this work, we demonstrate that NDR can occur in structures of atomic dimensions ( $\sim 1$  nm). These structures involve a tunnel diode configuration formed by specific surface sites and an STM tip. STM and scanning tunneling spectroscopy (4) are used to characterize these surface sites and measure their  $I$ - $V$  characteristics. We also present a simple model to explain NDR at the atomic level.

We have observed NDR in several surface chemical systems. In all cases, NDR developed at localized surface sites. Here we will discuss examples involving structures produced by the adsorption of boron on silicon, Si(111). This system is particularly well suited for the observation of NDR because

IBM Research Division, T. J. Watson Research Center, Yorktown Heights, NY 10598.